

## NEUROSYSTEMS

# Putative spinal interneurons mediating postural limb reflexes provide a basis for postural control in different planes

Pavel V. Zelenin, Li-Ju Hsu, Vladimir F. Lyalka, Grigori N. Orlovsky and Tatiana G. Deliagina

Department of Neuroscience, Karolinska Institute, SE-17177 Stockholm, Sweden

**Keywords:** postural networks, posture, rabbit, spinal interneurons

## Abstract

The dorsal-side-up trunk orientation in standing quadrupeds is maintained by the postural system driven mainly by somatosensory inputs from the limbs. Postural limb reflexes (PLRs) represent a substantial component of this system. Earlier we described spinal neurons presumably contributing to the generation of PLRs. The first aim of the present study was to reveal trends in the distribution of neurons with different parameters of PLR-related activity across the gray matter of the spinal cord. The second aim was to estimate the contribution of PLR-related neurons with different patterns of convergence of sensory inputs from the limbs to stabilization of body orientation in different planes. For this purpose, the head and vertebral column of the decerebrate rabbit were fixed and the hindlimbs were positioned on a platform. Activity of individual neurons from L5 to L6 was recorded during PLRs evoked by lateral tilts of the platform. In addition, the neurons were tested by tilts of the platform under only the ipsilateral or only the contralateral limb, as well as during in-phase tilts of the platforms under both limbs. We found that, across the spinal gray matter, strength of PLR-related neuronal activity and sensory input from the ipsilateral limb decreased in the dorsoventral direction, while strength of the input from the contralateral limb increased. A near linear summation of tilt-related sensory inputs from different limbs was found. Functional roles were proposed for individual neurons. The obtained data present the first characterization of posture-related spinal neurons, forming a basis for studies of postural networks impaired by injury.

## Introduction

In quadrupeds, the dorsal-side-up trunk orientation during standing is maintained due to the activity of the postural system. This closed-loop control system is driven by sensory signals and produces corrective motor responses that compensate for deviations from the stabilized orientation (Horak & Macpherson, 1996; Beloozerova *et al.*, 2003; Deliagina *et al.*, 2006b). The postural system relies mainly on somatosensory information from limb mechanoreceptors (Inglis & Macpherson, 1995; Deliagina *et al.*, 2000, 2006a, 2012; Beloozerova *et al.*, 2003; Stapley & Drew, 2009), although visual and vestibular information can also be used in some postural tasks (Horak & Macpherson, 1996).

Several studies have provided evidence that some important postural mechanisms for trunk stabilization persist in decerebrate animals (Bard & Macht, 1958; Musienko *et al.*, 2008; Honeycutt *et al.*, 2009; Honeycutt & Nichols, 2010). This preparation can thus be used for the analysis of underlying neuronal networks.

In a previous study (Musienko *et al.*, 2010), we characterized postural limb reflexes (PLRs) in the decerebrate rabbit, i.e., electromyogram (EMG) and force responses to anti-phase flexion and extension movements of the hindlimbs caused by tilts of a

supporting platform while the vertebral column and pelvis were rigidly fixed. It was suggested that PLRs in intact animals contribute to postural reactions (Musienko *et al.*, 2010; Deliagina *et al.*, 2012).

Recently, we revealed the spinal neurons presumably contributing to the generation of PLRs (Hsu *et al.*, 2012). According to their response to platform tilts, these neurons were divided into two groups: F neurons, activated during flexion of the ipsilateral limb, and E neurons, activated during extension of this limb). It was also demonstrated that the phase of modulation of a neuron was determined mainly by sensory input from the ipsilateral limb.

The first aim of the present study was to reveal trends in the spatial distribution of neurons with different parameters of PLR-related activity across the spinal gray matter. We found that, across the spinal gray matter, the background level of neuronal activity is relatively constant while the strength of the PLR-related modulation decreases in the dorsoventral direction.

The second aim of the present study was to perform a detailed characterization of sensory inputs to PLR-related neurons from the ipsilateral and contralateral limbs, as well as to estimate the contribution of neurons receiving different patterns of sensory inputs to the stabilization of body orientation in different planes. We found that the majority of neurons receive sensory inputs from both limbs, with the inputs being linearly summated. We also found that sensory inputs from the receptive field of a neuron (determined at rest) can be responsible for the tilt-related modulation only in some of the

Correspondence: Dr P. V. Zelenin, as above.  
E-mail: Pavel.Zelenin@ki.se

Received 27 June 2014, revised 1 October 2014, accepted 8 October 2014

neurons. Based on these new findings, a hypothesis about contributions of neurons with different patterns of sensory inputs to the control of body orientation in different planes is formulated.

A brief account of a part of this study has been published in abstract form (Zelenin *et al.*, 2012a,b).

## Materials and methods

Experiments were carried out on 20 adult New Zealand rabbits (weight 2.5–3.5 kg; both males and females). All experiments were carried out in accordance with the EU Directive 2010/63/EU on the protection of animals used for scientific purposes and were approved by the local ethical committee (Norra Djurförsöksetiska Nämnden) in Stockholm.

### Surgical procedures

The animal was injected with propofol (average dose 10 mg/kg, administered intravenously) for induction of anesthesia, which was continued with isoflurane (1.5–2.5%) delivered in O<sub>2</sub>. The trachea was cannulated. For all subsequent procedures, the animal was positioned in a metal frame with its head and vertebral column rigidly fixed (Fig. 1A). The spinal cord was exposed by laminectomy at segment L5. The dura mater was left intact, except for small holes (~1 mm<sup>2</sup>) through which recording electrodes were inserted. Four bipolar EMG electrodes were implanted into the hindlimb muscles. EMGs from *m. gastrocnemius lateralis* (ankle extensor), *m. vastus lateralis* (knee extensor) were recorded bilaterally to monitor PLRs

throughout the time course of the experiment and to confirm the satisfactory condition of the preparation. No quantitative analysis of EMGs was done in the present study.

The animal was then decerebrated at the precollicular–postmammary level (Musienko *et al.*, 2008). After decerebration, the anesthesia was discontinued. During the experiment, the rectal temperature and blood pressure were continuously monitored and kept at 37–38 °C and >90 mmHg (cuff blood pressure measurement device, petMAP, Ramsay Medical Inc., USA), respectively. To counteract loss of fluid and the subsequent loss of blood pressure, physiological Ringer solution was injected (10–20 mL, s.c., over the course of the experiment). Recordings began at least 1 h after cessation of anesthesia. The experiments were terminated by a lethal dose of anesthetic (sodium pentobarbital) followed by decapitation.

### Experimental design

The experimental design (Fig. 1A) and the method of induction of PLRs was similar to that described previously (Musienko *et al.*, 2010; Hsu *et al.*, 2012). In short, the head and vertebral column were rigidly fixed. The forelimbs were suspended in a hammock. The hindlimbs were hemi-flexed and positioned on a horizontal platform consisting of two parts, the right platform and the left platform. The limb configuration and the distance between the feet were similar to that observed in intact freely standing rabbits (Beloozerova *et al.*, 2003).

The platform as a whole, or its right or left parts separately, could be tilted periodically by rotation around the medial axis with an

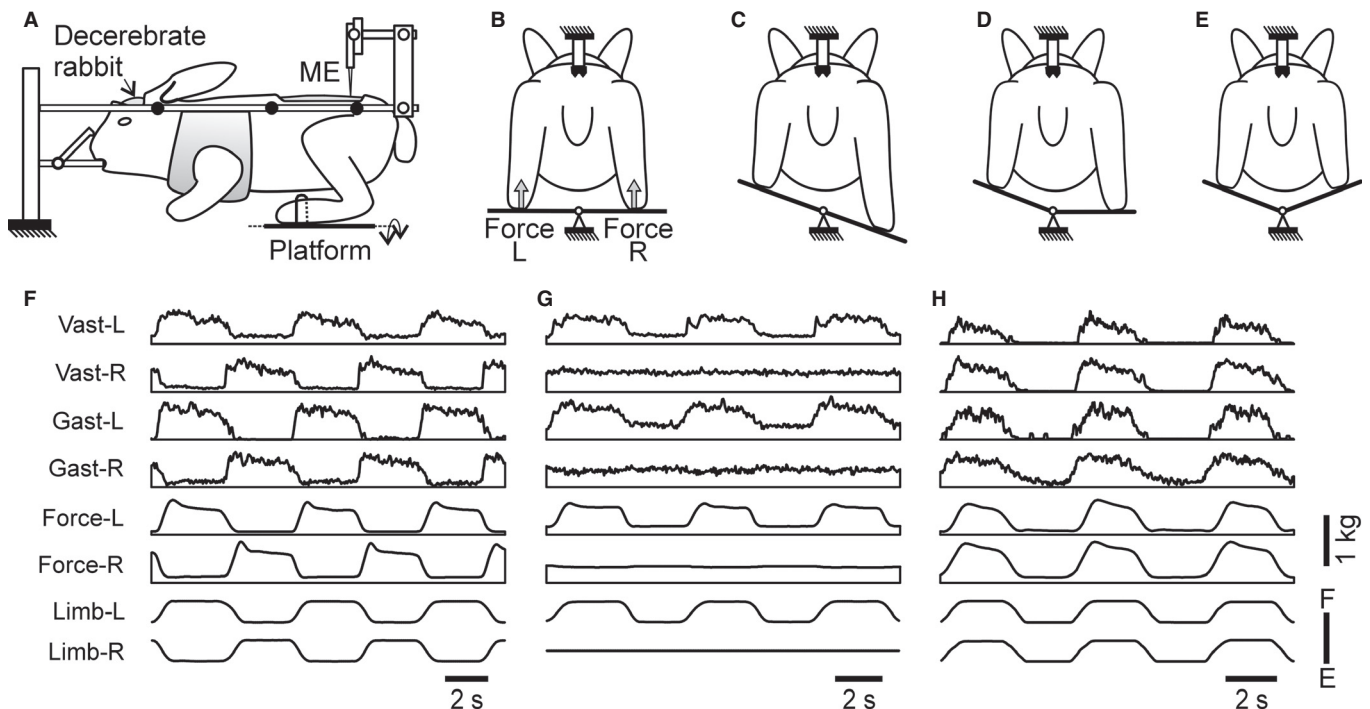


FIG. 1. Experimental design. (A) A decerebrate rabbit was positioned in a rigid frame, and its head and vertebral column were firmly fixed (points of fixation are indicated by black circles). (B) For testing postural limb reflexes (PLRs), the hindlimbs were positioned on a platform which could be periodically tilted (C and F) in the transverse plane as a whole, (D and G) its right and left parts separately or (E and H) both parts in-phase. Tilt of the whole platform caused flexion of one limb and extension of the other limb (C and F). Flexion–extension movements of the left and right limbs were monitored by mechanical sensors (Limb-L and Limb-R, respectively). The contact forces under the left and right limbs were measured by the force sensors (Force-L and Force-R in B). The PLRs were monitored by recording contact forces and EMGs of limb muscles when the whole platform (F), only its left part (G) or right part, or both parts in-phase (H) were tilted. The extensor muscles of the right (R) and left (L) limb were recorded: Vast, *m. vastus lateralis*; Gast, *m. gastrocnemius lateralis*. The activity of spinal neurons from L5–L6 was recorded with an extracellular microelectrode (ME in A).

amplitude of  $\pm 20^\circ$  (Fig. 1C–E). As the position of the hip joint was fixed, tilts of the whole platform led to flexion–extension movements of the hip, knee and ankle joints and near-vertical displacements of the distal point of the limb. The time trajectory of tilting the platform, and therefore the time trajectory of foot displacement, was trapezoidal with a period of  $\sim 6$  s (Fig. 1F–H); the transition between extreme positions lasted for  $\sim 0.5$ – $1$  s and each position was maintained for  $\sim 2$ – $2.5$  s. The flexion–extension movements of the left and right limbs were monitored by mechanical sensors (Limb-L and Limb-R in Fig. 1F–H). The contact forces under the limbs were measured by means of force sensors (Force-L and Force-R in Fig. 1B and F–H).

Tilt-related somatosensory stimulation (caused by loading and flexion of the limb on the side of the platform moving up, and unloading and extension of the limb on the side of the platform moving down) evoked PLRs. They included activation of extensors in the flexing limb and increase in its contact force, as well as inactivation of extensors in the extending limb and decrease in its contact force (Musienko *et al.*, 2008, 2010), as illustrated in Fig. 1F–H. A separate tilt of the left (Fig. 1G) or right platform evoked PLRs mainly in the ipsilateral limb (Musienko *et al.*, 2010).

### Neuronal recording

Spinal neurons were recorded extracellularly in segment L5–L6 using commercially available varnish-insulated tungsten electrodes (75  $\mu$ m shaft diameter; FHC, Bowdoin, ME, USA) with an impedance of 4–7 M $\Omega$ . We tried to explore the entire cross-section of the gray matter except for the area of motor nuclei, without bias (Portal *et al.*, 1991). The lateral and vertical co-ordinates of each neuron were marked on a map of the spinal cord cross-section (Shek *et al.*, 1986). Individual neurons were recorded during PLRs caused by periodical tilts of the whole platform, along with EMGs and ground reaction forces. To reveal tilt-related somatosensory inputs from the left and right limbs to individual PLR neurons, the majority of neurons were also recorded during separate tilts of the right and left platform (Fig. 1D). To assess the linearity of summation of sensory inputs to individual neurons, a subset of neurons was also recorded during in-phase tilts of the left and right parts of the platform (Fig. 1E).

To characterize the spatial sensitivity of PLR neurons in greater detail, a subset was recorded during tilt of the whole platform from  $20^\circ$  left to  $20^\circ$  right and then back to  $20^\circ$  left performed in steps of  $10^\circ$  (Fig. 5). During this test, each position was maintained for  $\sim 2$  s, and the transition between them lasted for  $\sim 1$  s.

Peripheral receptive fields were examined in some of the neurons. Stimuli included light brushing of hairs, light tapping of hairy skin, firm tapping on and palpation of muscle bellies (flexors and extensors of ankle, knee and hip, and abductors and adductors of hip) and tendons, pinching the skin with fingers, and in a few cases manual movements of joints. If a cutaneous input was observed then the responses from the underlying muscles were not taken into account. Stimuli that could potentially activate nociceptors (i.e. pinching or poking with sharp instruments) were not used.

### Data analysis

Signals from the microelectrode (neuronal activity) and the EMG electrodes, as well as from the platform position and force sensors, were amplified, digitized with sampling frequencies of 30 kHz (microelectrode), 10 kHz (EMGs) and 100 Hz (sensors), displayed on the screen, and saved to a computer disc by means of a data acquisition and analysis system (Power1401/Spike2, Cambridge

Electronic Design, Cambridge, UK). The EMG signals were rectified and smoothed (time constant, 100 ms).

Waveform analysis of neuronal activity was employed to discriminate and identify the spikes of a single neuron, using the Spike2 waveform-matching algorithm. Only neurons with a stable response and spike shape were used for analysis.

The analysis of neuronal activity is illustrated in Fig. 2A–D. As PLRs of individual limbs are usually caused by tilt-related somatosensory information from the same limb (Musienko *et al.*, 2010), when tilting either the entire platform or only the ipsilateral platform we considered the activity of all individual neurons in the movement cycle of the ipsilateral limb. The onset of the ipsilateral limb flexion was taken as the cycle onset (Fig. 2D). When only the contralateral platform was tilted, the cycle started at the onset of extension of the contralateral limb.

For each neuron, the raster of its spike activity in sequential cycles was obtained (Fig. 2C). The cycle was divided into 12 bins (Fig. 2D). Bins 1 and 2 corresponded to flexion of the ipsilateral limb, bins 3–6 to maintenance of the flexed position, bins 7 and 8 to extension of the limb and bins 9–12 to maintenance of the extended position. The firing frequency in each bin was calculated and averaged over the identical bins in all cycles at a given condition, and a phase histogram was generated (Fig. 2D). The mean frequency during flexion of ipsilateral limb (bins 1–6) and that during extension (bins 7–12) were compared. The larger and the smaller values were named the burst frequency ( $F_{\text{BURST}}$ ) and the interburst frequency ( $F_{\text{INTER}}$ ), respectively. The neuron was considered to be modulated by tilts if the difference between the mean burst frequency and mean interburst frequency was statistically significant (two-tailed Student's *t*-test,  $P < 0.05$ ).

Then we calculated the mean frequency  $F_M = (F_{\text{BURST}} + F_{\text{INTER}})/2$ , the depth of modulation  $\Delta F = F_{\text{BURST}} - F_{\text{INTER}}$ , and the coefficient of modulation  $K_{\text{MOD}} = 1 - F_{\text{INTER}}/F_{\text{BURST}}$ . To characterize the relative strength of the ipsilateral and the contralateral tilt-related somatosensory inputs to a neuron, we calculated the index of ipsilaterality  $\text{InIp} = (\Delta F_{\text{ipsi}} - \Delta F_{\text{contra}})/\max(\Delta F_{\text{ipsi}}, \Delta F_{\text{contra}})$ , where  $\Delta F_{\text{ipsi}}$  and  $\Delta F_{\text{contra}}$  were the depths of modulation during tilts of only ipsilateral or only contralateral platform. Obviously,  $\text{InIp} = +1$  if a neuron had only ipsilateral inputs,  $\text{InIp} = -1$  if a neuron had only contralateral inputs,  $\text{InIp} = 0$  if a neuron had ipsilateral and contralateral inputs of equal strength,  $\text{InIp} > 0$  if the ipsilateral input was stronger and  $\text{InIp} < 0$  if the contralateral input was stronger.

To reveal trends in the distribution of different parameters across the gray matter, 'heatmaps' for local mean were generated (Figs 3, 7 and 8). To calculate a value in the heatmap point with coordinates (*x*,*y*), we used measured values of a parameter for the neurons that were recorded in the vicinity of the point. The measured values were weighted depending on the distance *d* from (*x*,*y*) to the recording point [Gaussian weighting  $w(d) = \exp(-d^2/D^2)$  with the spatial constant  $D = 0.4$  mm].

All quantitative data in this study are presented as mean  $\pm$  SD. Two-tailed Student's *t*-test was used to characterize the statistical significance when comparing different means.

### Histological procedures

At the end of experiment, reference electrolytic lesions were made in the spinal cord. The spinal cord was fixed with a 10% formalin solution. Frozen sections of 30  $\mu$ m thickness were cut in the region of recording. The tissue was stained for Nissl substance with Cresyl violet. Positions of recording sites were estimated in relation to the lesions.

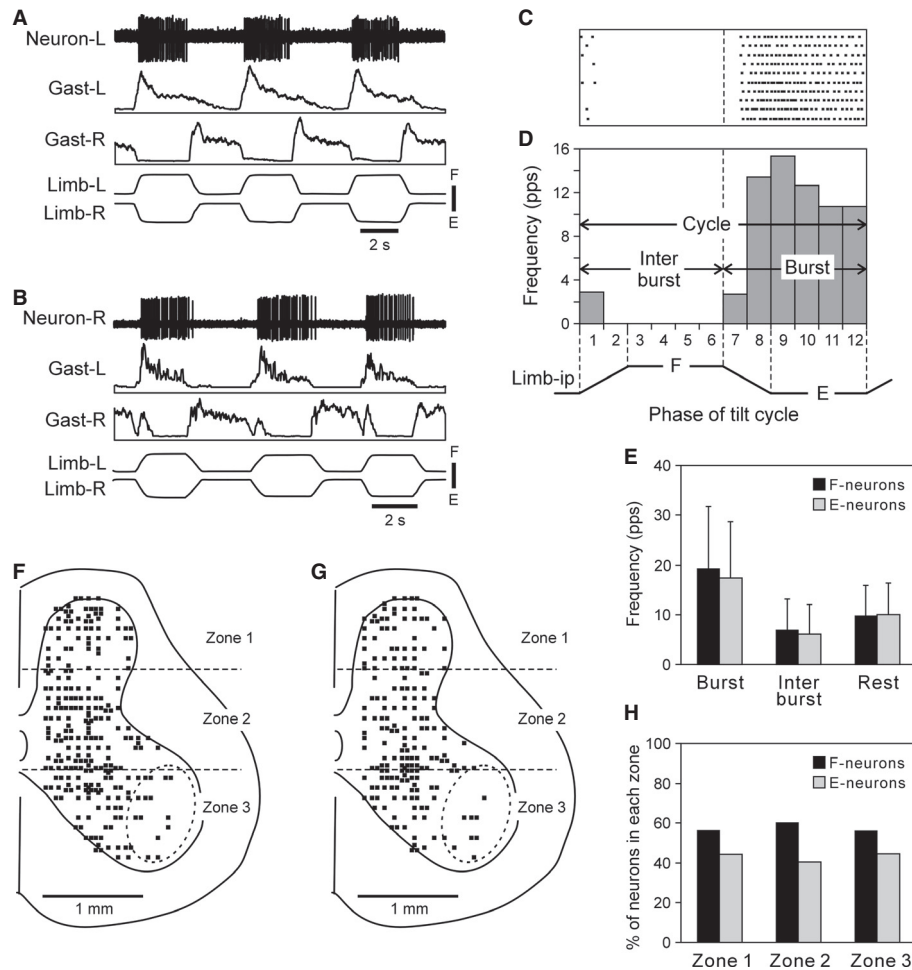


FIG. 2. Classification of responses of spinal neurons to platform tilts. (A and B) Two examples of activity of spinal neurons recorded during PLRs caused by tilts of the whole platform. One neuron was located on the left side of the spinal cord and activated during flexion of the left limb; it was classified as an F neuron (A). The other neuron was located on the right side and activated during extension of the right limb; it was classified as an E neuron (B). Abbreviations as in Fig. 1E. (C and D) Characterization of activity of the neuron presented in B. (C) A raster of responses of an E neuron in 10 sequential movement cycles of the ipsilateral limb. (D) A histogram of spike activity (for the neuron shown in C) in different phases (1–12) of the cycle of movement (F, flexion; E, extension) of the ipsilateral limb (Limb-ip). The halves of the cycle with higher (E, bins 7–12) and lower (F, bins 1–6) neuronal activity were designated as ‘Burst’ and ‘Interburst’ periods, respectively. (E) The mean and SD values of the burst frequency (Burst), interburst frequency (Interburst) and discharge frequency with a non-tilting (horizontal) platform (Rest) are shown for F neurons ( $n = 142$ ) and E neurons ( $n = 118$ ) (only neurons with noticeable activity at rest were considered). The difference between Burst and Rest, as well as between Interburst and Rest values, was statistically significant for both E and F neurons ( $P < 0.0001$ , paired  $t$ -test). (F and G) Positions of all recorded F neurons ( $n = 248$ , F) and E neurons ( $n = 187$ , G) on the cross-section of the spinal cord. The area of motor nuclei is indicated by dotted line. Three zones of the gray matter are indicated: dorsal (zone 1), intermediate (zone 2), and ventral (zone 3). (H) Relative numbers of F neurons and E neurons in different zones of the gray matter. The numbers of neurons recorded in zones 1, 2, 3 were  $n = 107$ , 157 and 167, respectively.

## Results

### Distribution of neurons with different parameters of PLR-related activity

Altogether, we recorded 435 neurons whose activity correlated with PLRs caused by the whole-platform tilts. (Neurons without clear tilt-related activity were not systematically recorded and therefore were not included in the analysis.) According to the phase of response in the tilt cycle of the ipsilateral limb, all modulated neurons were divided into two groups. The F neurons had a higher firing frequency in the flexion phase than in the extension phase (as the neuron in Fig. 2A). During the flexion phase, the extensor muscles were activated to counteract the tilt; therefore, the F neurons were active in-phase with the extensor muscles of the ipsilateral limb. By contrast, E neurons were more active in the extension phase (as the neuron in Fig. 2B). In some neurons, the spontaneous activity at rest

was recorded. For neurons of both groups (142 F and 118 E neurons), the burst frequency was significantly higher and the interburst frequency was significantly lower than their firing frequency with non-tilted (horizontal) platform (Rest) (Fig. 2E), suggesting that, in both F and E neurons, the burst is determined by excitatory input and the interburst by inhibitory input. F neurons and E neurons constituted 57% and 43% of all modulated neurons, respectively. The distributions of F neurons and E neurons on the cross-section of the spinal cord are shown in Fig. 2F and G, respectively. The overwhelming majority of neurons were situated outside the motor nuclei (indicated by dotted lines) and thus they could be considered putative interneurons.

From Fig. 2F and G, one can see that both types of neurons are represented across the entire extent of the gray matter. To roughly characterize the distribution of neurons, we divided the cross-section into three zones (1–3) and calculated the relative number of



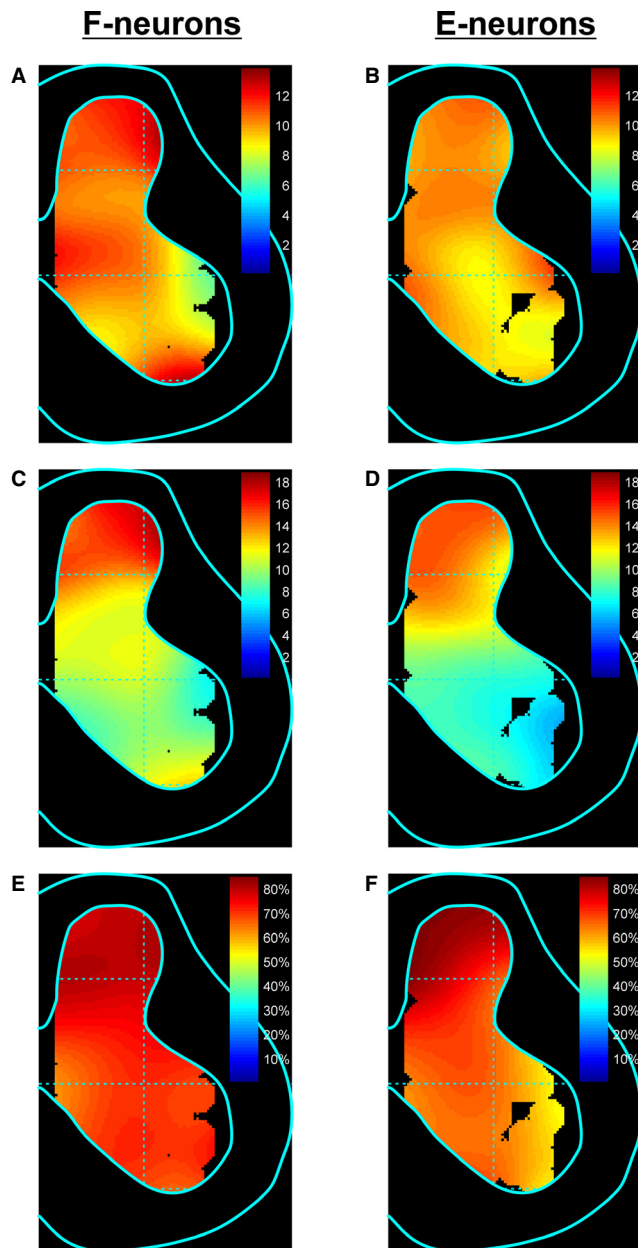


Fig. 3. Distribution of activity characteristics of F neurons and E neurons across the gray matter. (A, C and E) Heatmaps showing the distributions of (A) the mean frequency, (C) the depth of modulation and (E) the coefficient of modulation for F neurons ( $n = 248$ ). (B, D and F) Heatmaps showing the distributions of (B) the mean frequency, (D) the depth of modulation and (F) the coefficient of modulation for E neurons ( $n = 187$ ). The color in each point indicates the local population mean (see Materials and Methods).

F neurons and E neurons in each of the zones. As shown in Fig. 2H, F neurons prevailed over E neurons in all zones, with an approximate proportion 3 : 2.

To reveal trends in the distribution of neurons with different parameters of PLR-related activity across the gray matter of the spinal cord, we calculated the mean values of different parameters ( $F_M$ ,  $\Delta F$  and  $K_{MOD}$ ) for local populations of neurons, and presented them as heatmaps (see Materials and Methods). Figure 3 shows these maps for F neurons (Fig. 3A, C and E) and E neurons (Fig. 3B, D and F). There were no clear 'hot spots' on  $F_M$  (Fig. 3A and B) or  $K_{MOD}$  maps (Fig. 3E and F). The difference between the

mean values of  $F_M$  in the populations of F neurons and E neurons located in different areas of the gray matter did not exceed 2–4 Hz (Fig. 3A and B).  $K_{MOD}$  was similar (~75%) in the populations of F neurons located in different areas of the gray matter (Fig. 3E), but in E neurons  $K_{MOD}$  gradually decreased from 85% to 60% in the dorsoventral direction (Fig. 3F). In both F neurons and E neurons,  $\Delta F$  gradually decreased two-fold in the dorsoventral direction (Fig. 3C and D, respectively).

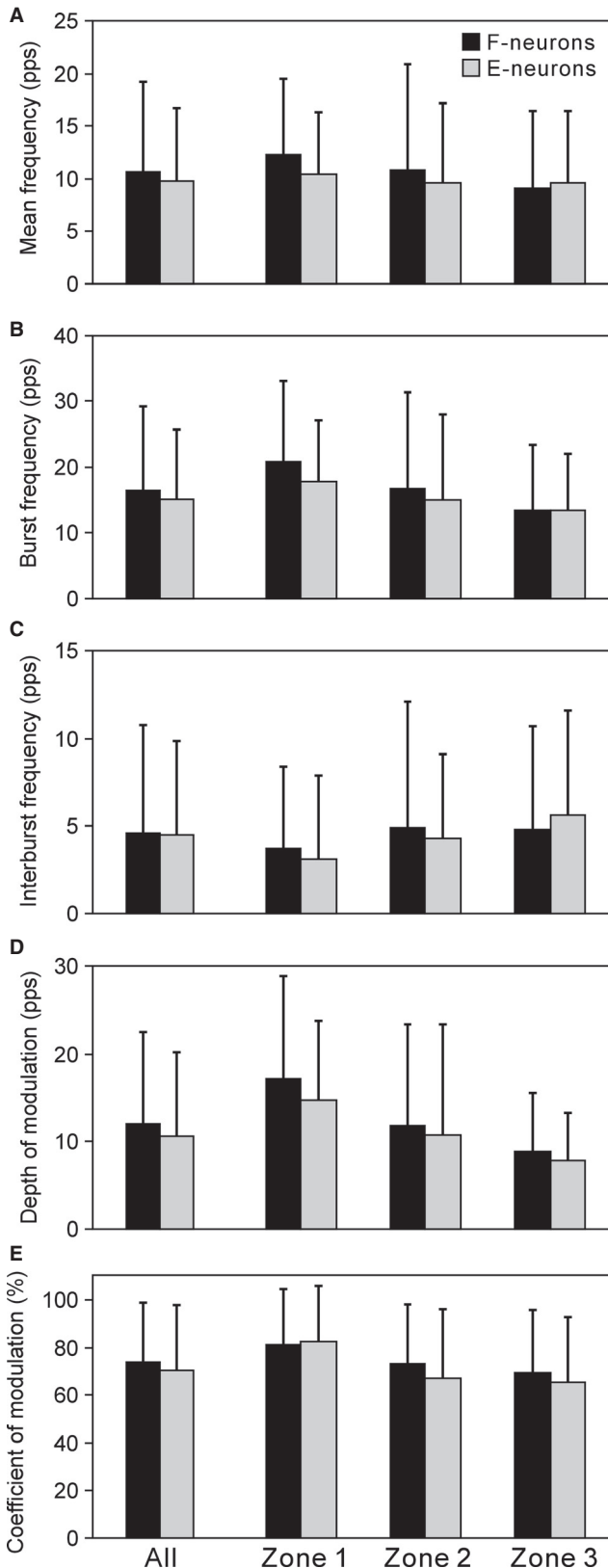
The mean value and dispersion of different parameters characterizing F neurons and E neurons ( $F_M$ ,  $F_{BURST}$ ,  $F_{INTER}$ ,  $\Delta F$ ,  $K_{MOD}$ ) are shown in Fig. 4 for all neurons, as well as separately for neurons in each of three zones of the gray matter. Although individual values were highly variable, the mean values of these parameters in each zone were similar for F neurons and E neurons. In E neurons,  $F_M$  values were similar in all three zones, but in F neurons they progressively decreased from zone 1 to zone 3 (Fig. 4A). In both F and E neurons, the values of  $\Delta F$  (Fig. 4D) progressively decreased from zone 1 to zone 3 due to both a decrease in  $F_{BURST}$  (Fig. 4B) and an increase in  $F_{INTER}$  (Fig. 4C). In F neurons,  $K_{MOD}$  values were similar in all three zones, but in E neurons they progressively decreased from zone 1 to zone 3 (Fig. 4E).

#### Zones of spatial sensitivity of PLR-related neurons

To reveal zones of spatial sensitivity of PLR-related neurons, 137 neurons (72 F neurons and 65 E neurons) were recorded during tilt of the whole platform from 20° left to 20° right and in the opposite direction, performed in sequential steps of 10° (Fig. 5). Two examples of response patterns observed in this test are shown in Fig. 5A and B. The neuron in Fig. 5A responded during those tilts which caused transition from the extended to the flexed configuration of the ipsilateral limb; this neuron was practically silent during tilts in the opposite direction, thus displaying high directional sensitivity. The responses appeared first at the threshold angle of 0° (horizontal orientation) and increased with further flexion, thus showing monotonic angle dependence. The frequency during tilting was higher than at the stationary position; thus the neuron exhibited both dynamic and static components in its response to each angular step.

Another example of responses in this test is presented in Fig. 5B. This neuron displayed monotonic angle dependence during tilt of the platform in any direction and thus had no directional sensitivity; it had only a static component of response. Altogether, 110 out of 137 tested neurons displayed the monotonic angle dependence during tilt either in only one or in both directions. Directional sensitivity was displayed by 99 out of 110 neurons, and 71 out of 110 had a dynamic component of response. As one can see from Table 1, the majority of neurons responded in the whole range of tested tilt angles and only a slim minority had a narrow angular zone of sensitivity. Out of the most frequently encountered neurons (with both dynamic and static components of response, and with clear directional sensitivity), 31 neurons belonged to F group and 40 neurons to E group. The other 26 F neurons and 13 E neurons had only static responses. The majority of these neurons (21 F neurons and nine E neurons) had directional sensitivity.

Six out of 137 tested neurons had approximately the same activity during all tilts except for the tilt towards the extreme angle in one direction, as the neuron in Fig. 5C. Eight other neurons responded to tilts towards the extreme angle in any direction. An example of such a neuron is shown in Fig. 5D. Finally, 13 of 137 tested neurons had very complex responses and could not be categorized to any of the aforementioned groups.



#### PLR-related neurons with different combinations of sensory inputs from ipsilateral and contralateral limbs

In the previous study (Hsu *et al.*, 2012), on a small sample of neurons ( $n = 48$ ) we have shown that PLR-related neurons can receive different combinations of tilt-related sensory inputs from the hind-

FIG. 4. Population characteristics of F neurons and E neurons. The mean and SD values of (A) the mean frequency, (B) the burst frequency, (C) the interburst frequency, (D) the depth of modulation and (E) the coefficient of modulation for F neurons and E neurons are shown. These values are shown for the entire F and E populations (All), as well as for their sub-populations located in different areas (zones 1–3 of the gray matter; see Fig. 2F–G). Statistically significant differences were found: in A, between values for F neurons in zones 1 and 3 ( $P < 0.05$ ); in B, between values for F neurons and values for E neurons in zones 1 and 3 ( $P < 0.001$  and  $P < 0.05$ , respectively); in C, between values for E neurons in zones 1 and 3 ( $P < 0.05$ ); in D, between values for F neurons in zones 1 and 2 ( $P < 0.01$ ) and in zones 2 and 3 ( $P < 0.05$ ), as well as between values for E neurons in zones 1 and 3 ( $P < 0.001$ ); in E, between values for F neurons in zones 1 and 2 ( $P < 0.05$ ) and in zones 1 and 3 ( $P < 0.01$ ), as well as between values for E neurons in zones 1 and 2 ( $P < 0.01$ ) and in zones 1 and 3 ( $P < 0.001$ ).

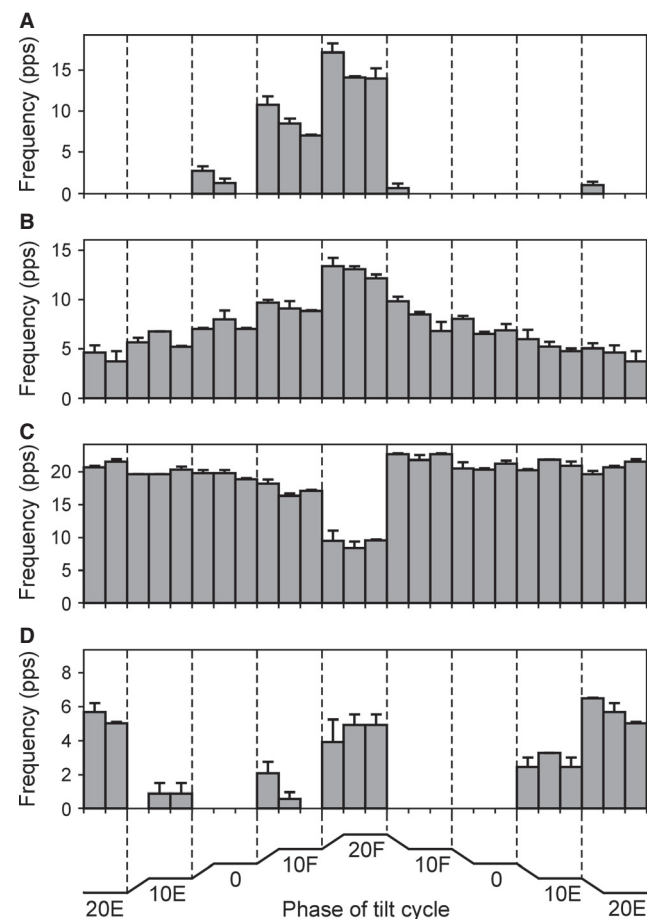


FIG. 5. Zones of spatial sensitivity of PLR-related neurons. (A–D) Examples of responses of spinal neurons to tilts of the whole platform from the position of 20°E (extension of the ipsilateral limb) to 20°F (flexion of the ipsilateral limb) and in the opposite direction, performed in sequential steps of 10°. (A) A neuron with directional sensitivity and both dynamic and static components of the response. (B) A neuron without directional sensitivity and with only a static component of the response. (C) A neuron that was inhibited at extreme flexion. (D) A neuron that responded mainly during tilts of the platform away from the horizontal (0) position. (See Results for details).

limbs. The aim of the present study was to quantitatively characterize sensory inputs from each of the limbs to individual F and E neurons, as well as to reveal the distribution of neurons with different inputs over the cross-section of the gray matter. For this purpose, in addition to examining responses from tilts of the entire

TABLE 1. Proportions of neurons with different thresholds for dynamic and static components of response

Threshold	Dynamic response		Static response	
	<i>n</i>	%	<i>n</i>	%
−10°	51 out of 71	72	70 out of 110	64
0°	15 out of 71	21	18 out of 110	16
+10°	4 out of 71	6	18 out of 110	16
+20°	1 out of 71	1	4 out of 110	4

Threshold is the angle at which the dynamic or static component of the response appeared during tilt of the whole platform from −20° to +20° performed in sequential steps of 10°. Positive angle values indicate the tilt of the platform to the side of maximal response and negative angle values indicate tilt to the opposite side. Numbers and percentages of neurons with a particular threshold for dynamic and static components of the response are indicated.

platform we recorded responses to separate tilts of its right and left parts in 307 neurons (Fig. 1D).

The diagram in Fig. 6A quantitatively characterizes the strength of sensory inputs from ipsilateral and contralateral limbs to individual neurons. Type 1 (T1) neurons responded to tilts of the ipsilateral but not the contralateral platform (as in the example shown in Fig. 6B) and are situated on the horizontal axis (diamonds). The neurons with positive and negative values of frequency difference belong to ET1 (E neurons of type T1; gray diamonds) and FT1 (F neurons of type T1; black diamonds) sub-groups, respectively. Type 2 (T2) neurons responded to tilts of the contralateral but not the ipsilateral platform (as the neuron in Fig. 6C) and are situated on the vertical axis (triangles). The neurons with positive and negative values of frequency difference belong to ET2 (gray triangles) and FT2 (black triangles) sub-groups, respectively. Type 3 (T3) neurons received complementary inputs from the limbs. They responded to flexion of the ipsilateral limb and extension of the contralateral limb, or to extension of the ipsilateral limb and flexion of contralateral limb. An example of a T3 neuron is shown in Fig. 6D. In Fig. 6A, T3 neurons (circles) are situated in the upper right and lower left quadrants [ET3 (gray circles) and FT3 (black circles) subgroups, respectively]. Finally, Type 4 (T4) neurons received opposing inputs from the two limbs, as a neuron in Fig. 6F. It responded to flexion of the ipsilateral limb during tilts of the ipsilateral platform and to flexion of the contralateral limb during tilts on the contralateral platform. In Fig. 6A, T4 neurons (squares) are situated in the upper left and lower right quadrants containing neurons of both FT4 (black squares) and ET4 (gray squares) sub-groups, respectively. T3 neurons and T4 neurons were scattered across the whole plane, demonstrating that relative strengths of inputs from the ipsi-limb and contralateral limb to individual PLR neurons were very diverse.

Figure 6F shows the relative number of neurons of different types, as well as the proportion of F and E neurons in each of the types. T1 neurons were the most numerous (117 out of 307 neurons, or 38%). T2 neurons were much less numerous (47 neurons, or 15%). T3 and T4 neurons were almost equal in number (22 and 25%, respectively). The proportion of F and E neurons was ~ 2 : 1 in T1 and T3 neurons, and ~ 1 : 1 in T2 and T4 neurons. The locations of individual neurons on gray-matter cross-sections are shown in Fig. 8C for FT1–FT4 neurons, and in Fig. 8D for ET1–ET4 neurons.

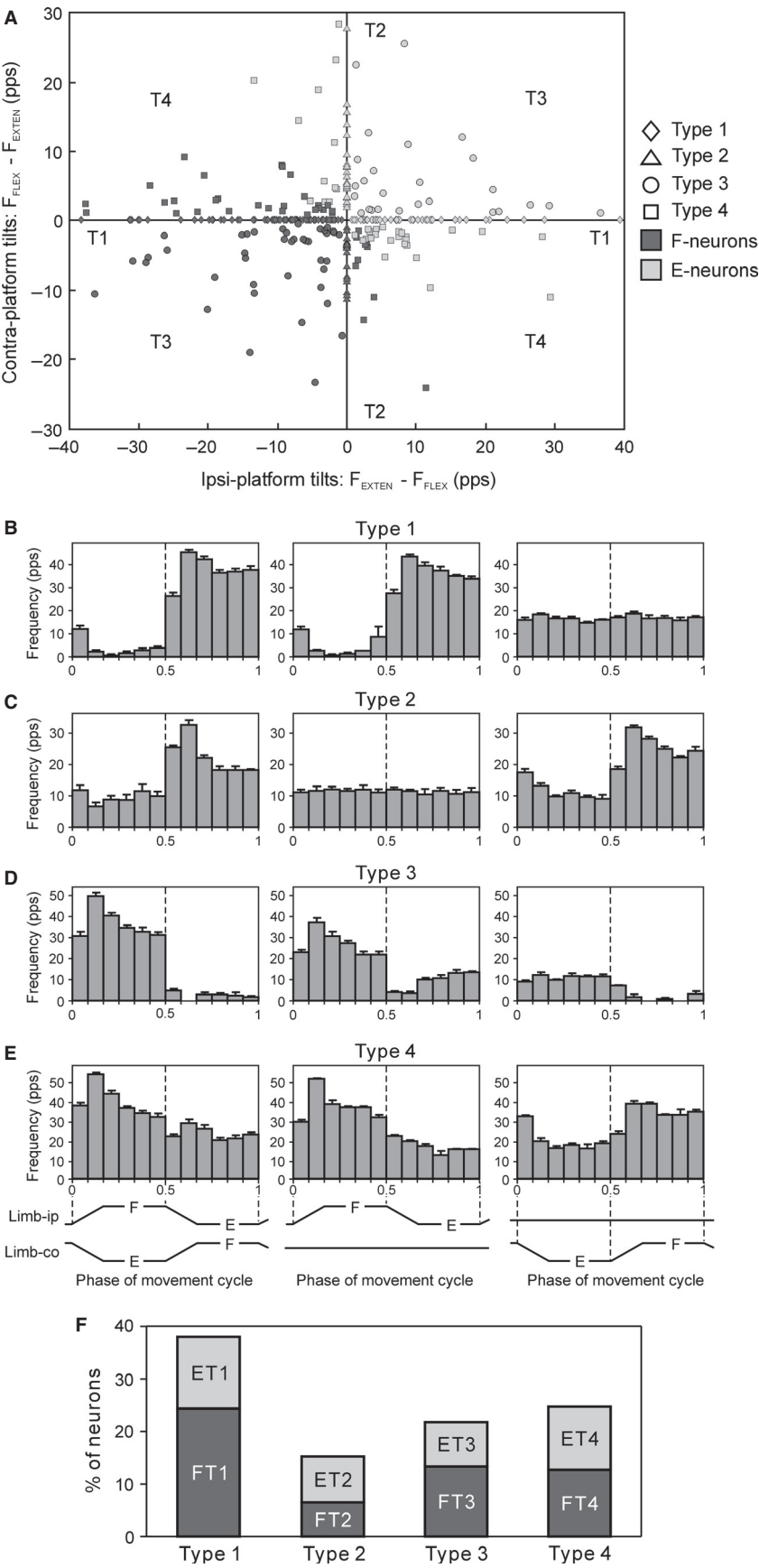
To characterize the strength of ipsilateral and contralateral inputs to neurons located in different areas of the gray matter, we plotted the depth of modulation  $\Delta F$  for individual F neurons and E neurons in different locations during tilts of only the ipsilateral platform or only the contralateral platform, and then the corresponding heatmaps for the local means of the  $\Delta F$  values were generated for F neurons (Fig. 7A and C) and E neurons (Fig. 7B and D).

The average value of the depth of modulation caused by input from the ipsilateral limb in F neurons gradually decreased in the dorsoventral direction, from 15 to 5 pulse per second (pps) (Fig. 7A), suggesting a respective decrease in the strength of the ipsilateral input. The contralateral input to F neurons on average was much weaker than the ipsilateral input (compare Fig. 7A and C), and its strength slightly increased in the dorsoventral direction, from 1 to 4 pps (Fig. 7C). However, in some neurons, the contralateral input could be rather strong, with  $\Delta F > 20$  pps.

In general, the ipsilateral input to E neurons was slightly weaker and the contralateral input was slightly stronger than to F neurons (compare Fig. 7B and D with A and C). E neurons with the strongest ipsilateral input were located in the medial part of the dorsal horn and in the lateral part of the intermediate area of the gray matter (Fig. 7B). The strength of ipsilateral input to E neurons (as in F neurons) decreased in the dorsoventral direction (compare Fig. 7B and A). E neurons with the strongest contralateral input were located in the ventral part of the dorsal horn (Fig. 7D). In some neurons in this area the contralateral input could be very strong, causing the depth of modulation to be  $>50$  pps. The highest variability in the strength of the ipsilateral and contralateral inputs to E neurons, and strength of the ipsilateral input to F neurons, was observed in the intermediate area of the gray matter, at a depth of 1.0–1.5 mm.

To evaluate the relative strength of the ipsilateral input and contralateral input, we calculated the index of ipsilaterality, *InIp* (see Materials and Methods). F neurons and E neurons with different values of *InIp* were dispersed across the gray matter (Fig. 8C and D, respectively). On the average, *InIp* decreased in the dorsoventral direction in both F neurons (Fig. 8A) and E neurons (Fig. 8B). However, in F neurons the prevalence of ipsilateral input was stronger than in E neurons. In the ventral part of the dorsal horn and in the intermediate area *InIp* was +0.8 in F neurons versus +0.2 in

FIG. 6. Classification of PLR-related neurons according to tilt-related sensory inputs from ipsilateral and contralateral limbs. (A) Values of sensory inputs from the ipsilateral and contralateral limbs to individual neurons ( $n = 307$ ). The difference in mean frequencies during ipsilateral limb extension and ipsilateral limb flexion caused by tilts of the ipsilateral platform only (abscissa) is plotted versus the difference in mean frequencies during contralateral limb flexion and contralateral limb extension caused by tilts of the contralateral platform only (ordinate). The neurons were divided into four types according to the pattern of their modulation [T1, inputs from only the ipsilateral limb (diamonds); T2, inputs from only the contralateral limb (triangles); T3, complementary inputs from the two limbs (circles); T4, opposite inputs from the two limbs (squares)]. F and E neurons are shown by black and gray symbols, respectively. (B–E) Histograms of activity of four neurons with different patterns of responses to tilts of the whole platform, ipsilateral platform and contralateral platform [phases of movement cycle (F, flexion; E, extension) for the ipsilateral limb (Limb-ip) and contralateral limb (Limb-co) are indicated]. (B) Type 1 neuron (ET1) had similar responses to tilts of the whole platform and of the ipsilateral platform only (activation during extension of the ipsilateral limb); it did not respond to tilts of the contralateral platform. (C) Type 2 neuron (ET2) had similar responses to tilts of the whole platform and of the contralateral platform (excitation during flexion of the contralateral limb); it did not respond to tilts of the ipsilateral platform. (D) Type 3 neuron (FT3) had complementary responses to tilts of the ipsilateral platform (excitation during flexion of the ipsilateral limb) and of the contralateral platform (excitation during extension of the contralateral limb). (E) Type 4 neuron (FT4) had opposite responses to tilts of the ipsilateral platform and of the contralateral platform (excitation during flexion of any limb). (F) Relative numbers of T1, T2, T3 and T4 neurons. Bars for the neurons of each type are divided into two parts to show proportion of F neurons and E neurons.





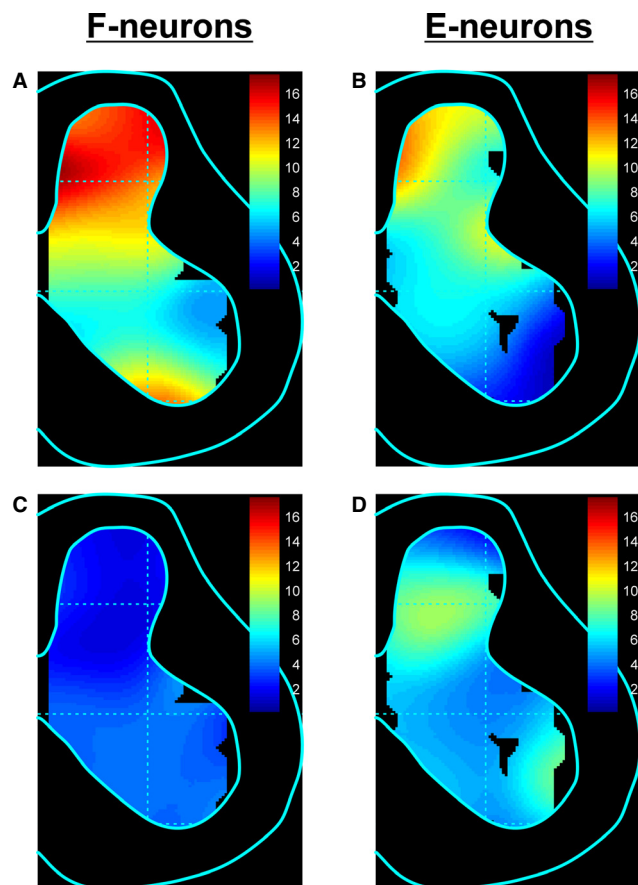


FIG. 7. Distribution of the values of ipsilateral and contralateral sensory inputs to F neurons and to E neurons across the gray matter. A–D, The heatmaps showing the distribution of the depth of modulation during tilts of the ipsilateral platform only (A, B) and contralateral platform only (C, D) for F neurons ( $n = 175$ ) and E neurons ( $n = 132$ ), respectively. The color in each point indicates the local population mean (see Methods).

E neurons. Finally, in the ventral part of the ventral horn, the ipsilateral input dominated ( $InIp \sim +0.4$ ) in F neurons. By contrast, E neurons in this area had ipsilateral and contralateral inputs that were similar ( $InIp \sim 0$ ).

As one can see in Fig. 8C and D, FT1- and ET1 neurons (with  $InIp = +1$ ) tended to reside in the dorsal and intermediate areas of the gray matter, while FT2 and ET2 neurons (with  $InIp = -1$ ) tended to reside in the intermediate and ventral areas. T3 and T4 neurons (subgroups FT3, ET3, FT4 and ET4) were scattered across the gray matter, and neurons with predominating ipsilateral input and contralateral input could be intermingled.

#### Summation of sensory inputs from ipsilateral and contralateral limbs

While the phase and the depth of modulation of T1 and T2 neurons were determined by tilt-related sensory input from only ipsilateral or only contralateral limb, respectively, modulation of T3 and T4 neurons was a result of the interaction of sensory inputs from two limbs. To assess the linearity of summation of the tilt-related sensory inputs from the hindlimbs, 53 T3 neurons and 56 T4 neurons were recorded during tilts of the ipsilateral platform part only, tilts of the contralateral platform part only, anti-phase tilts of the two platform parts (tilts of the whole platform), and in-phase tilts of the

two platform parts (Fig. 1E). For each of these tests, we subtracted the mean frequency ( $F_M$ ) from the burst frequency ( $F_{BURST}$ ) and interburst frequency ( $F_{INTER}$ ), thus providing the response frequency:  $\delta F = F - F_M$ . The response frequency  $\delta F$  was treated as a function of the hindlimb lengths  $X_{ipsi}$  and  $X_{contra}$ .  $X_{ipsi}$  was equal to +1 when the ipsilateral hindlimb was extended, -1 when it was flexed and 0 when the support platform under the limb was horizontal. The same values were used for  $X_{contra}$ . For example,  $\delta F(+1, -1)$  was the response frequency when the whole platform was tilted ipsilaterally (the ipsilateral limb extended, the contralateral limb flexed), or  $\delta F(0, +1)$  was the response frequency during extension of the contralateral limb only, or  $\delta F(-1, -1)$  was the response frequency during simultaneous flexion of both limbs. Then we calculated the linear fit for the  $\delta F(X_{ipsi}, X_{contra})$  data points together with the coefficient of determination  $R^2$ , the latter indicating goodness of the fit. It was found that in 77% of neurons the summation was strongly linear with  $R^2 \geq 0.95$ , and in the other 23% of neurons the summation was rather linear with  $R^2 \geq 0.85$ .

#### Relation between neuronal responses to tilts and their receptive fields

Somatosensory receptive fields were found in 247 of 286 neurons tested (86%). In the majority of the neurons (229 out of 247, 93%) the receptive fields were 'deep': the neurons responded to palpation of muscles or to movements of joints, but not to stimulation of the fur or skin alone (there were only 18 such neurons, nine of which also had input from muscles). In 119 out of 247 neurons (48%) only one afferent input (that is a response either from only one muscle or from only one area of the skin) was found, while the rest (52%) received more than one input. In 173 out of 247 neurons (70%), the receptive field was restricted to the ipsilateral limb, in 18 neurons (7%) to the contralateral limb, and in the other 56 neurons (23%) the receptive field included both limbs. The majority of neurons (75%) had excitatory receptive fields, 3% were inhibited by passive manipulation of the hindlimbs, and in 22% of neurons both excitatory and inhibitory afferent inputs were found.

For 211 neurons with 'deep' receptive fields, which were tested by tilts of the separate platform sides and by the whole platform, we compared responses of a neuron to tilts with afferent signals that the neuron presumably receives from its receptive field during tilts. One could expect that tilt of the platform would activate stretch and load receptors in extensors of the flexing limb, and those in flexors of the extending limb. If the input from the receptive field were responsible for the neuronal reactions to tilts one could expect activation of neurons of the FT1-subgroup with stimulation of ipsilateral extensors, ET1 with stimulation of ipsilateral flexors, FT2 with stimulation of contralateral extensors, ET2 with stimulation of contralateral flexors, FT3 with stimulation of ipsilateral extensors and contralateral flexors, ET3 with stimulation of ipsilateral flexors and contralateral extensors, FT4 with stimulation of ipsilateral extensors and contralateral extensors, and ET4 with stimulation of ipsilateral flexors and contralateral flexors.

However, it was found that only 49 out of 211 neurons (23%) had corresponding receptive fields (Table 2). Seven per cent of neurons had afferent inputs that could be responsible for their reaction to tilt, but they also had mismatching inputs (for example, excitatory inputs from the antagonistic muscles of one limb). Twenty seven out of 108 (25%) T3 and T4 neurons had the receptive field only on one limb, which could be responsible for their reaction to tilt of only the ipsilateral platform or only the contralateral platform. Eighteen per cent of T3 and T4 neurons, in addition to afferent inputs

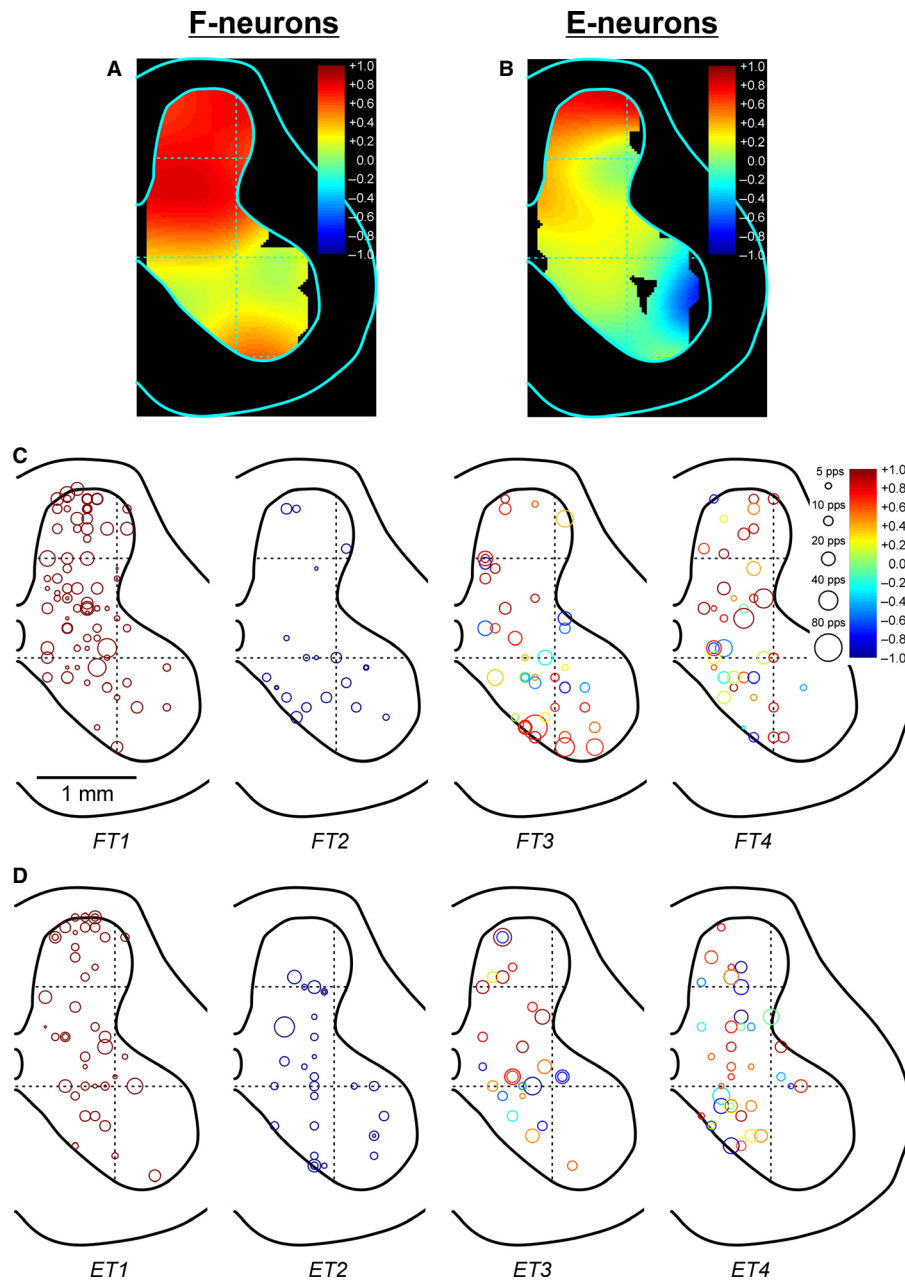


FIG. 8. Distribution of relative value of the ipsilateral and contralateral sensory inputs to F neurons and to E neurons across the gray matter. (A–D) Distribution of the index of ipsilaterality (see Materials and Methods) that characterizes the relative contribution of inputs from the ipsilateral limb and contralateral limb to modulation of neurons. The index is equal to +1 when modulation is caused by input from the ipsilateral limb only. It is equal to –1 when modulation is caused by input from the contralateral limb only. It is equal to 0 when inputs from both limbs have the same magnitude. (A and B) Heatmaps showing the local population mean for the index of ipsilaterality for F and E neurons, respectively. (C and D) Positions of different types of (C) F neurons and (D) E neurons in the gray matter. The circle diameter and color indicate the mean frequency and the index of ipsilaterality of the neuron, respectively.

that could be responsible for their reaction to tilts, also had mismatching afferent inputs. Finally, modulation of 101 out of 211 neurons (48%) could not be explained by input from the receptive fields.

## Discussion

### Characterization of PLR-related neurons

In the present study we characterized 435 neurons from spinal segments L5–L6, with activity correlated to PLRs. We suggest that

these neurons receive (mono- or polysynaptic) tilt-related sensory information and contribute to the generation of PLRs.

The exact identity of the recorded neurons remains unknown. However, there are several lines of evidence suggesting that they are interneurons (segmental, propriospinal, involved in the spinal postural feedback loop, or ascending, involved in the supraspinal loop) driven by proprioceptive, mainly muscle, afferents. First, most recorded neurons were located outside of the area of motor nuclei. Therefore they are most probably not motoneurons. Second, for 62% of 307 neurons that were tested for inputs from individual limbs a contralateral input was revealed (Fig. 8C and D). Many of

TABLE 2. Relation between neuronal responses to tilts and to receptive field stimulation

Subgroups	Matched		Partly matched		Matched and mismatched		Partly matched and mismatched		Mismatched		Total	
	<i>n</i>	%	<i>n</i>	%	<i>n</i>	%	<i>n</i>	%	<i>n</i>	%	<i>n</i>	%
FT1	25	41	0		9	15	0		27	44	61	29
FT2	1	33	0		0		0		2	67	3	1
FT3	3	11	7	27	1	4	4	15	11	43	26	12
FT4	1	3	12	34	0		7	20	15	43	35	17
ET1	14	47	0		1	3	0		15	50	30	14
ET2	5	56	0		0		0		4	45	9	4
ET3	0		4	15	1	4	4	15	17	66	26	12
ET4	0		4	19	3	14	4	19	10	48	21	10
Total	49	23	27	13	15	7	19	9	101	48	211	100

Numbers and percentages of neurons in each sub-group are indicated. Matched, reaction to tilts can be explained by stimulation of receptive field; Partly matched, stimulation of receptive field can explain a part of reaction to tilts; Matched and mismatched, stimulation of a part of the receptive field can explain reaction to tilts, but input from another part of receptive field mismatches; Mismatched, reaction to tilts cannot be explained by stimulation of receptive field. Percentages in the last column and the last row are calculated for the whole population. Percentages elsewhere are calculated for individual subgroups.

these neurons were located in the most dorsal layers of the gray matter. Also, 52% of the neurons for which receptive fields were found had more than one source of sensory input (e.g., two different muscles, or a muscle and a skin area, etc.). Thus these neurons could not be the afferent fibers traversing the gray matter. Third, in the vast majority of the tested neurons (93%), the receptive fields were 'deep' (muscle- or joint-related). Only 7% of the neurons had cutaneous inputs. The former number could be an underestimate as we did not take into account responses to stimulation of muscles under cutaneous receptive fields.

According to the phase of their activity in the tilt cycle, all neurons were divided into two groups: F neurons were modulated in-phase with extensor motoneurons of the ipsilateral limb, whereas E neurons were modulated in anti-phase. F and E neurons were intermingled and scattered across the whole cross-section of the gray matter (Fig. 2F and G). The latter is not surprising as tilt-related somatosensory signals are most likely transmitted by group I and II afferents from the limb muscles, and spinal interneurons receiving inputs from these afferents are located in different areas of the gray matter (Jankowska *et al.*, 2002, 2009; Edgley *et al.*, 2003; Jankowska, 2008; Bannatyne *et al.*, 2009). F neurons were slightly more numerous in all zones of the gray matter (Fig. 2H). These results are similar to those obtained in our previous studies, in which small samples of PLR-related neurons were recorded (Hsu *et al.*, 2012; Zelenin *et al.*, 2013).

In both F and E neurons, the burst frequency was significantly higher, and the interburst frequency was significantly lower, than their firing frequency with the non-tilted platform (Fig. 2E), suggesting that the burst is determined by excitatory input and the interburst by inhibitory input.

The analysis of spatial distribution of neurons with different activity characteristics has shown that the mean frequency was similar in different areas of the gray matter (Fig. 3A and B), suggesting that spinal circuits located in these areas are similarly activated. The depth of modulation decreased in the dorsoventral direction (Figs 3C and D and 4D) due to a decrease in  $F_{\text{BURST}}$  and an increase in  $F_{\text{INTER}}$  (Fig. 4B and C). We found neither any clear lateromedial changes in the distribution of different parameters nor any clear peaks or troughs in this distribution (Fig. 3).

F and E groups are not homogeneous. They could contain segmental and propriospinal interneurons as well as the ascending tract neurons, some of which may be implicated in supraspinal postural feedback

loops while others may be involved in sensory perception. The ascending neurons may include, e.g., spinocerebellar tract neurons, which receive inputs from group I and II afferents (Jankowska & Puczyńska, 2008; Jankowska & Hammar, 2013). However, one can assume that at least some of the recorded F and E neurons are pre-motor interneurons that activate and inhibit extensor motoneurons, respectively. Such pre-motor interneurons with inputs from group I and II afferents have been found in the lumbosacral enlargement (Cavallari *et al.*, 1987; Jankowska *et al.*, 2005; Bannatyne *et al.*, 2006, 2009).

The majority of both F and E neurons responded throughout the range of tested tilt angles, had directional sensitivity and exhibited both dynamic and static responses (Table 1), suggesting their contribution to both dynamic and static components of PLRs (Musienko *et al.*, 2010) in the whole range of tilt angles.

The neurons with directional sensitivity are most probably driven by group Ia muscle afferents, and the neurons with only static responses to tilts and without directional sensitivity by group II muscle afferents. The areas of terminations of Ia and II afferents in the gray matter are largely overlapping. Both Ia and II afferents terminate in Rexed laminae VI, VII and IX. Laminae VI and VII contain different interneurons receiving monosynaptic input from group Ia, group II or both groups of afferents; these are excitatory interneurons with ipsilateral, bilateral or contralateral projections, and inhibitory interneurons projecting ipsilaterally (Bannatyne *et al.*, 2006). Some of these excitatory and inhibitory interneurons (both with ipsilateral and contralateral projections) are premotor interneurons (Edgley & Jankowska, 1987b; Jankowska *et al.*, 2009). Group Ia and II afferents also affect neurons of spinocerebellar pathways (Hongo *et al.*, 1983a,b; Jankowska & Puczyńska, 2008; Jankowska & Hammar, 2013). Most likely the population of spinal neurons with directional sensitivity and the population of neurons with only static responses to tilts and without directional sensitivity revealed in the present study contain all these types of neurons. In addition, group II afferents terminate in laminae IV, V and VIII (Edgley & Jankowska, 1987a). Lamina IV contains excitatory and lamina V inhibitory interneurons with monosynaptic inputs from group II afferents (Bannatyne *et al.*, 2006). Excitatory neurons project ipsilaterally and inhibitory ones both ipsilaterally and contralaterally. Some of them have synapses on motoneurons. Finally, lamina VIII contains commissural interneurons which receive input from group II afferents and affect motoneurons and interneurons (Edgley *et al.*, 2003; Jankowska, 2008; Jankowska *et al.*, 2009).

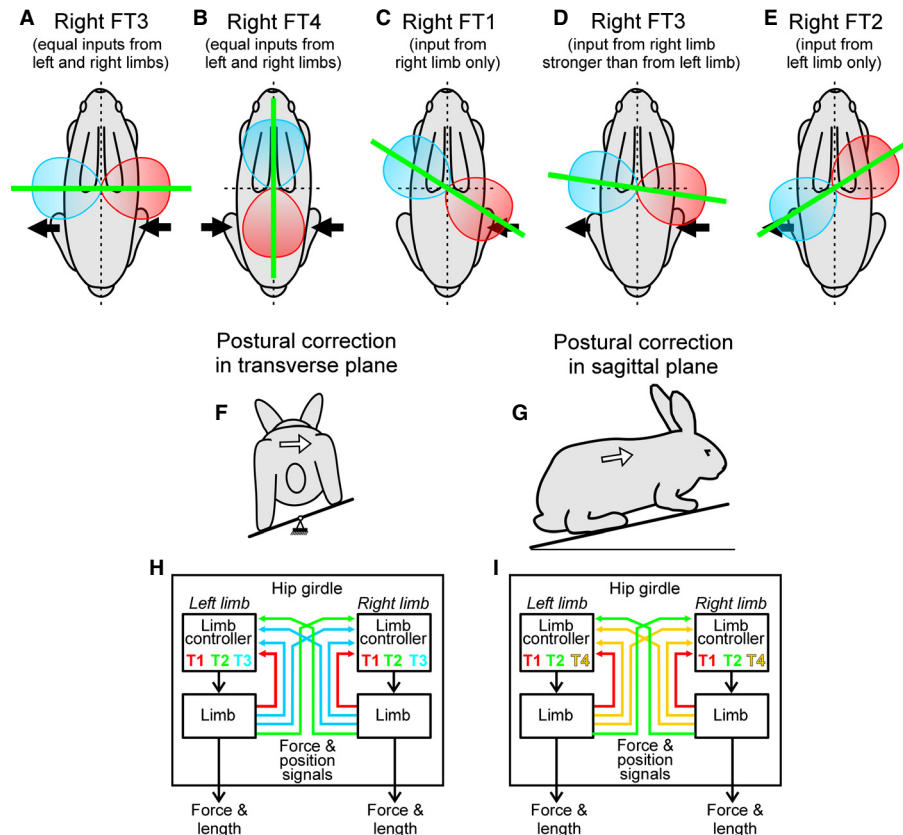


FIG. 9. Contributions of different types of spinal neurons to stabilization of body orientation in different planes (hypothesis). (A–E) Hypothetical tuning curves and preferred planes of tilts for different types of PLR-related neurons. Arrows towards and away from the midline indicate activation of a neuron with loading and with unloading of the limb, respectively. The size of an arrow is proportional to the value of the neuronal response. The red and blue shapes are the hypothetical tuning curves of the neurons (the response value is determined by the extent of loading or unloading of the left and right limbs, which depends on the tilt plane orientation). Red color indicates excitation, blue indicates inhibition. For each neuron, there is a direction of the strongest response and therefore a preferred plane of responses (thick green line): transverse in A, sagittal in B, diagonal in C–E. (A) Hypothetical tuning curve and preferred plane of a right FT3 neuron with equally strong responses to loading of the right limb and unloading of the left limb (see Discussion for explanation). (B) Preferred tilt plane of a right FT4 neuron with equally strong responses to loading of any hindlimb is the sagittal one (as the neuron is maximally activated during nose-up tilts and inactivated during nose-down tilt in this plane). Tilts in the transverse plane do not affect the neuron's activity because excitatory effects of ipsilateral limb loading are cancelled by inhibitory effects of contralateral limb unloading. (C) A right FT1 neuron is activated by ipsilateral tilt in the transverse plane, and by nose-up tilt, as both of these tilts load the limb. However, the maximal response (and thus preferred plane) can be expected during diagonal tilts, with the right caudal corner of the platform moving down, producing maximal right hindlimb loading. (D) A right FT3 neuron with a stronger response to ipsilateral limb loading than to contralateral limb unloading has the preferred tilt plane oriented between the preferred planes of the neurons presented in A and C. (E) A right FT2 neuron receiving input only from the contralateral limb responds maximally during the diagonal tilt (the caudal left corner of the platform moves up). (F and G) Postural reactions to tilts of the support surface in (F) the transverse plane and (G) the sagittal plane. An arrow shows the direction of the corrective movement caused by the tilt. (H and I) Orientation of hindquarters in (H) the transverse plane and (I) the sagittal plane is stabilized by many parallel reflex chains that involve neurons of different types. These types of neurons (T1–T4) are indicated by the same color as their sensory inputs from the hindlimbs. (See Discussion for explanations).

Most likely the population of spinal neurons with only static responses to tilts and without directional sensitivity contains also these neuronal types located in laminae IV, V and VIII.

#### Sources of modulation of PLR-related neurons

According to sources of their modulation (the ipsilateral or/and contralateral hindlimbs), all PLR-related neurons were divided into four types. In T1 neurons (38%), modulation was determined by sensory input from the ipsilateral limb only, suggesting their involvement in the intra-limb coordination, i.e., in the generation of corrective limb movements in response to sensory inputs from the same limb (Fig. 9H and I). In intact animals, a substantial part of corrective limb movements is generated by this mechanism (Deliagina *et al.*, 2006a).

In T2 neurons (15%), modulation was determined by sensory input from the contralateral limb only. They may include commis-

sural interneurons (with sensory input from the contralateral limb) involved in the intra-limb coordination (together with T1 neurons, Fig. 9H,I), and ipsilaterally projecting neurons (with sensory input from the contralateral limb) involved in the inter-limb coordination. In the intact animal, somatosensory signals from the contralateral limb contribute to the generation of corrective limb movements (Deliagina *et al.*, 2006a). In decerebrate animals, signals transmitted by T2 neurons with contralateral input could be sub-threshold, resulting in the weakness of PLRs during contralateral limb tilts (Fig. 1G; see also Musienko *et al.*, 2010).

T3 neurons (with complementary inputs from the two limbs; 22%) and T4 neurons (with opposite inputs; 25%) are most likely involved in the inter-limb coordination during postural corrections.

Neurons with ipsilateral and contralateral inputs were intermingled and scattered across the gray matter (Fig. 8C and D). In most F neurons, the contralateral input was much weaker than the



ipsilateral input (Fig. 7A and C). In E neurons, the contralateral input was stronger and the ipsilateral input was slightly weaker than those in F neurons (Fig. 7: compare B and D with A and C, respectively). One possible explanation for this finding could be a lesser activation of limb afferents signaling limb extension than those signaling limb flexion due to the hemiflexed limb configuration in both E and F phases. Previously, interneurons with ipsilateral inputs from the group I and II afferents and ipsilateral projections were found in different areas of the gray matter (Bannatyne *et al.*, 2006, 2009). Commissural neurons with ipsilateral inputs from the group I and II afferents and with terminals in different areas of the contralateral gray matter (which could mediate input from the contralateral limb) were also described (Bannatyne *et al.*, 2006, 2009; Jankowska *et al.*, 2009).

In 23% of recorded neurons (Table 2), the response pattern corresponded well to the pattern that one could expect provided the neuron was driven by its receptive field input. However, in 48% of neurons, input from the receptive field could not be responsible for their reactions to tilts. One can suggest that, in these neurons, when the platform tilt simultaneously activates receptors of several muscles, input from the receptive field observed at rest is complemented or replaced by other sensory inputs.

#### Functional role of PLR-related neurons in postural control

In the present study, all spinal neurons were divided into four types (T1–T4) depending on the combination of sensory inputs from individual limbs causing their modulation (Fig. 6). What are possible functional roles of these different types? Tilts in the transverse plane used in this study produced loading and unloading of the limbs. Apparently, a tilt in any other plane will also change the loading of the left and right limbs in different proportion. We found that summation of tilt-related sensory inputs from the two hindlimbs was almost linear. One can therefore predict how neurons of different types will respond to tilts of the intact animal in different planes, and thus suggest their contribution to the generation of PLRs stabilizing trunk orientation in these planes. This is illustrated in Fig. 9A–E.

For example, if a right FT3 neuron has equally strong responses to loading of the right limb and unloading of the left limb (as indicated in Fig. 9A by inward and outward arrows of the same size), the neuron will be maximally activated with right tilt in the transverse plane, and maximally inactivated with left tilt in that plane. Tilts in the sagittal plane, when both hindlimbs are loaded or unloaded together, will produce little or no change in the activity of this neuron because excitatory effects of sensory input caused by right limb loading will be cancelled by inhibitory effect of sensory input caused by left limb loading. Tilts in the diagonal plane will cause responses of intermediate value. Figure 9A shows schematically a tuning curve of this neuron, i.e., the magnitude of neuronal response as a function of the tilt plane orientation (red, excitation; blue, inhibition), as well as the plane orientation at the maximal response (preferred plane, green line). Thus, this neuron will have a maximal contribution to the generation of PLRs with tilts in the transverse plane. Figure 9B–E shows tuning curves and preferred planes for right FT1–FT4 neurons with different strengths of sensory inputs from hindlimbs (see Fig. 9B–E legend for explanation).

To obtain the tuning curve for a particular type of the right E neurons, the tuning curve for the corresponding type of F neurons should be rotated by 180° in the horizontal plane.

Thus, we suggest that directional tuning of spinal neurons is essential for the generation of PLRs. Previously, directional tuning

was observed in the activity of different muscles during postural reactions to stance perturbations (Macpherson, 1988; Macpherson & Fung, 1999), and in neurons of the dorsal spinocerebellar tract to the foot trajectory (Bosco & Poppele, 1996, 1997).

The population of spinal neurons exposed in this study is presumably involved in population coding of commands for postural corrections in any vertical plane. Roughly, corrections in the transverse plane (arrow in Fig. 9F) are caused by T1–T3 neurons (Fig. 9H). Corrections in the sagittal plane (arrow in Fig. 9G) are caused by T1, T2 and T4 neurons (Fig. 9I).

One can suggest that the directional tuning of each individual spinal neuron to sensory inputs matches the motor effects that this neuron produces, i.e., the motor effects of each individual neuron counteract the postural disturbances that activate the neuron. Thus, PLR-related neurons are the key elements of the feedback loops participating in the stabilization of body orientation in a number of planes, with the largest contribution in the neuron's preferred plane. Such matching has been previously demonstrated for the command reticulospinal neurons eliciting postural reactions in the lamprey (Zelenin *et al.*, 2007), as well as for the nociceptive withdrawal reflex in the rat (Schouenborg, 2008).

Thus, we suggest that orientation of the hindquarters is stabilized by many parallel reflex chains that contain PLR-related neurons of different types. These postural reflex chains could be the targets of descending commands for voluntary changes of posture transmitted by the corticospinal (Beloozerova *et al.*, 2005; Karayannidou *et al.*, 2008), rubrospinal (Zelenin *et al.*, 2010) and other descending systems.

To conclude, in the present study a large population of putative spinal interneurons contributing to the generation of PLRs has been characterized and classified into groups according to the source of the tilt-related sensory inputs. The revealed groups present not a thorough but rather a primary classification that must be further elaborated in future studies. A hypothesis about the role of different types and groups of PLR-related neurons for postural stabilization in different planes has been proposed. To prove or to reject the proposed hypothesis, one needs to correlate the tilt-related sensory input to a recorded neuron with the motor output of the neuron, as has been done in simpler nervous systems (Deliagina *et al.*, 1999; Zelenin *et al.*, 2007). This will be a goal of our future studies.

#### Acknowledgements

This work was supported by grants from NIH (R01 NS-064964), from the Christopher & Dana Reeve Foundation (DA-1001-2), from the Swedish Research Council (no. 11554 to T.G.D. and no. 21076 to P.V.Z.), and by a grant from Ministry of Education in the Taiwanese Government to L.-J.H. The authors are grateful to Dr R. Hill and Dr K. Dougherty for valuable comments on the manuscript.

#### Abbreviations

E neurons, neurons with a higher firing frequency in the extension phase than in the flexion phase; EMG, electromyogram; ET1, E neurons of type T1; ET2, E neurons of type T2; ET3, E neurons of type T3; ET4, E neurons of type T4; F neurons, neurons with a higher firing frequency in the flexion phase than in the extension phase;  $F_{BURST}$ , burst frequency;  $F_{INTER}$ , inter-burst frequency;  $F_M$ , mean frequency; FT1, F neurons of type T1; FT2, F neurons of type T2; FT3, F neurons of type T3; FT4, F neurons of type T4;  $InIp$ , index of ipsilaterality;  $K_{MOD}$ , coefficient of modulation; PLR, postural limb reflex; pps, pulse per second; T1, Type 1 (neurons responding to tilts of the ipsilateral but not the contralateral platform); T2, Type 2 (neurons responding to tilts of the contralateral but not the ipsilateral platform); T3, Type 3 (neurons receiving complementary inputs from the limbs; they respond to flexion of the ipsilateral limb and extension of the contralateral

limb, or to extension of the ipsilateral limb and flexion of contralateral limb); T4, Type 4 (neurons receiving opposing inputs from the two limbs; they respond to flexion of any limb or extension of any limb caused by platform tilts);  $\Delta F$ , depth of modulation;  $\Delta F_{\text{contra}}$ ,  $\Delta F$  of only contralateral platform;  $\Delta F_{\text{ipsi}}$ ,  $\Delta F$  of only ipsilateral platform.

## References

- Bannatyne, B.A., Edgley, S.A., Hammar, I., Stecina, K., Jankowska, E. & Maxwell, D.J. (2006) Different projections of excitatory and inhibitory dorsal horn interneurons relaying information from group II muscle afferents in the cat spinal cord. *J. Neurosci.*, **26**, 2871–2880.
- Bannatyne, B.A., Liu, T.T., Hammar, I., Stecina, K., Jankowska, E. & Maxwell, D.J. (2009) Excitatory and inhibitory intermediate zone interneurons in pathways from feline group I and II afferents: differences in axonal projections and input. *J. Physiol.*, **587**, 379–399.
- Bard, P. & Macht, M.B. (1958) The behavior of chronically decerebrate cats. In Wolstenholme, G.E.W. & O'Connor, C.M. (Eds), *Neurological Basis of Behavior*. Churchill, London, pp. 55–71.
- Beloozerova, I.N., Zelenin, P.V., Popova, L.B., Orlovsky, G.N., Grillner, S. & Deliagina, T.G. (2003) Postural control in the rabbit maintaining balance on the tilting platform. *J. Neurophysiol.*, **90**, 3783–3793.
- Beloozerova, I.N., Sirota, M.G., Orlovsky, G.N. & Deliagina, T.G. (2005) Activity of pyramidal tract neurons in the cat during postural corrections. *J. Neurophysiol.*, **93**, 1831–1844.
- Bosco, G. & Poppele, R.E. (1996) Temporal features of directional tuning by spinocerebellar neurons: relation to limb geometry. *J. Neurophysiol.*, **75**, 1647–1658.
- Bosco, G. & Poppele, R.E. (1997) Representation of multiple kinematic parameters of the cat hindlimb in spinocerebellar activity. *J. Neurophysiol.*, **78**, 1421–1432.
- Cavallari, P., Edgley, S.A. & Jankowska, E. (1987) Post-synaptic actions of mid-lumbar interneurons on motoneurons of hind-limb muscles in the cat. *J. Physiol.*, **389**, 675–689.
- Deliagina, T.G., Orlovsky, G.N., Selverston, A.I. & Arshavsky, Y.I. (1999) Neuronal mechanisms for the control of body orientation in Clione. I. Spatial zones of activity of different neuron groups. *J. Neurophysiol.*, **82**, 687–699.
- Deliagina, T.G., Beloozerova, I.N., Popova, L.B., Sirota, M.G., Swadlow, H., Grant, G. & Orlovsky, G.N. (2000) Role of different sensory inputs for maintenance of body posture in sitting rat and rabbit. *Motor Control*, **4**, 439–452.
- Deliagina, T.G., Sirota, M.G., Zelenin, P.V., Orlovsky, G.N. & Beloozerova, I.N. (2006a) Interlimb postural coordination in the standing cat. *J. Physiol.*, **573**, 211–224.
- Deliagina, T.G., Orlovsky, G.N., Zelenin, P.V. & Beloozerova, I.N. (2006b) Neural bases of postural control. *Physiology*, **21**, 216–225.
- Deliagina, T.G., Zelenin, P.V. & Orlovsky, G.N. (2012) Physiological and circuit mechanisms of postural control. *Curr. Opin. Neurobiol.*, **22**, 646–652.
- Edgley, S.A. & Jankowska, E. (1987a) Field potentials generated by group II muscle afferents in the middle lumbar segments of the cat spinal cord. *J. Physiol.*, **385**, 393–413.
- Edgley, S.A. & Jankowska, E. (1987b) An interneuronal relay for group I and II muscle afferents in the midlumbar segments of the cat spinal cord. *J. Physiol.*, **389**, 647–674.
- Edgley, S.A., Jankowska, E., Krutki, P. & Hammar, I. (2003) Both dorsal and lamina VIII interneurons contribute to crossed reflexes from group II muscle afferents. *J. Physiol.*, **552**, 961–974.
- Honeycutt, C.F. & Nichols, T.R. (2010) The decerebrate cat generates the essential features of the force constraint strategy. *J. Neurophysiol.*, **103**, 3266–3273.
- Honeycutt, C.F., Gottschall, J.S. & Nichols, T.R. (2009) Electromyographic responses from the hindlimb muscles of the decerebrate cat to horizontal support surface perturbations. *J. Neurophysiol.*, **101**, 2751–2761.
- Hongo, T., Jankowska, E., Ohno, T., Sasaki, S., Yamashita, M. & Yoshida, K. (1983a) Inhibition of dorsal spinocerebellar tract cells by interneurons in upper and lower lumbar segments in the cat. *J. Physiol. (Lond.)*, **342**, 145–159.
- Hongo, T., Jankowska, E., Ohno, T., Sasaki, S., Yamashita, M. & Yoshida, K. (1983b) The same interneurons mediate inhibition of dorsal spinocerebellar tract cells and lumbar motoneurons in the cat. *J. Physiol. (Lond.)*, **342**, 161–180.
- Horak, F. & Macpherson, J. (1996) Postural orientation and equilibrium. In Shepard, J. & Rowell, L. (Eds), *Handbook of Physiology. Exercise: Regulation and Integration of Multiple Systems*. Oxford UP, New York, pp. 255–292.
- Hsu, L.-J., Zelenin, P.V., Orlovsky, G.N. & Deliagina, T.G. (2012) Effects of galvanic vestibular stimulation on postural limb reflexes and neurons of spinal postural network. *J. Neurophysiol.*, **108**, 300–313.
- Inglis, J.T. & Macpherson, J.M. (1995) Bilateral labyrinthectomy in the cat: effects on the postural response to translation. *J. Neurophysiol.*, **73**, 1181–1191.
- Jankowska, E. (2008) Spinal interneuronal networks in the cat: elementary components. *Brain Res. Rev.*, **57**, 46–55.
- Jankowska, E. & Hammar, I. (2013) Interactions between spinal interneurons and ventral spinocerebellar tract neurons. *J. Physiol.*, **591**, 5445–5451.
- Jankowska, E. & Puczyńska, A. (2008) Interneuronal activity in reflex pathways from group II muscle afferents is monitored by dorsal spinocerebellar tract neurons in the cat. *J. Neurosci.*, **28**, 3615–3622.
- Jankowska, E., Slawinska, U. & Hammar, I. (2002) On organization of a network in pathways from group II muscle afferents in feline lumbar spinal segments. *J. Physiol.*, **542**, 301–314.
- Jankowska, E., Edgley, S.A., Krutki, P. & Hammar, I. (2005) Functional differentiation and organization of feline midlumbar commissural interneurons. *J. Physiol.*, **565**, 645–658.
- Jankowska, E., Bannatyne, B.A., Stecina, K., Hammar, I., Cabaj, A. & Maxwell, D.J. (2009) Commissural interneurons with input from group I and II muscle afferents in feline lumbar segments: neurotransmitters, projections and target cells. *J. Physiol.*, **587**, 401–418.
- Karayannidou, A., Deliagina, T.G., Tamarova, Z.A., Sirota, M.G., Zelenin, P.V., Orlovsky, G.N. & Beloozerova, I.N. (2008) Influences of sensory input from the limbs on feline corticospinal neurons during postural responses. *J. Physiol.*, **586**, 247–263.
- Macpherson, J.M. (1988) Strategies that simplify the control of quadrupedal stance. II. Electromyographic activity. *J. Neurophysiol.*, **60**, 218–231.
- Macpherson, J.M. & Fung, J. (1999) Weight support and balance during perturbed stance in the chronic spinal cat. *J. Neurophysiol.*, **82**, 3066–3081.
- Musienko, P.E., Zelenin, P.V., Lyalka, V.F., Orlovsky, G.N. & Deliagina, T.G. (2008) Postural performance in decerebrate rabbit. *Behav. Brain Res.*, **190**, 124–134.
- Musienko, P.E., Zelenin, P.V., Orlovsky, G.N. & Deliagina, T.G. (2010) Facilitation of postural limb reflexes with epidural stimulation in spinal rabbits. *J. Neurophysiol.*, **103**, 1080–1092.
- Portal, J.J., Corio, M. & Viala, D. (1991) Localization of the lumbar pools of motoneurons which provide hindlimb muscles in the rabbit. *Neurosci. Lett.*, **124**, 105–107.
- Schouenborg, J. (2008) Action-based sensory encoding in spinal sensorimotor circuits. *Brain Res. Rev.*, **57**, 111–117.
- Shek, J.W., Wen, G.Y. & Wisniewski, H.M. (1986) *In Atlas of the Rabbit Brain and Spinal Cord*. Karger, New York.
- Stapley, P. & Drew, T. (2009) The pontomedullary reticular formation contributes to the compensatory postural responses observed following removal of the support surface in the standing cat. *J. Neurophysiol.*, **101**, 1334–1350.
- Zelenin, P.V., Orlovsky, G.N. & Deliagina, T.G. (2007) Sensory-motor transformation by individual command neurons. *J. Neurosci.*, **27**, 1024–1032.
- Zelenin, P.V., Beloozerova, I.N., Sirota, M.G., Orlovsky, G.N. & Deliagina, T.G. (2010) Activity of red nucleus neurons in the cat during postural corrections. *J. Neurosci.*, **30**, 14533–14542.
- Zelenin, P.V., Hsu, L.-J., Lyalka, V.F., Orlovsky, G.N. & Deliagina, T.G. (2012a) Spinal interneurons mediating postural limb reflexes. *2012 FENS Forum in Barcelona*. 131.09.
- Zelenin, P.V., Hsu, L.-J., Lyalka, V.F., Orlovsky, G.N. & Deliagina, T.G. (2012b) Heterogeneity of spinal interneurons mediating postural limb reflexes. *Soc. Neurosci. Abstr.*, **38**, 08.
- Zelenin, P.V., Lyalka, V.F., Hsu, L.-J., Orlovsky, G.N. & Deliagina, T.G. (2013) Effects of reversible spinalization on individual spinal neurons. *J. Neurosci.*, **33**, 18987–18998.